Author Manuscript

Author Manuscript

Author Manuscript

Author Manuscript

HHS Public Access

Author manuscript

*Biomaterials*. Author manuscript; available in PMC 2018 November 01.

Published in final edited form as:

*Biomaterials*. 2017 November ; 144: 144–154. doi:10.1016/j.biomaterials.2017.08.029.

# Degradable Bioadhesive Nanoparticles for Prolonged Intravaginal Delivery and Retention of Elvitegravir

**Muneeb Mohideen**[†,1], **Elias Quijano**[†,1], **Eric Song**[1], **Yang Deng**[1], **Gauri Panse**[2], **Wei Zhang**[3], **Meredith R. Clark**[3], and **W. Mark Saltzman**[#,1]

[1]Department of Biomedical Engineering, Yale University, New Haven, CT 06511, USA

[2]Department of Dermatology, Yale University, New Haven, CT 06520, USA

[3]CONRAD, Department of Obstetrics and Gynecology, Eastern Virginia Medical School, Arlington, VA 22209, USA

## Abstract

New methods for long-lasting protection against sexually transmitted disease, such as the human immunodeficiency virus (HIV), are needed to help reduce the severity of STD epidemics, especially in developing countries. Intravaginal delivery of therapeutics has emerged as a promising means to provide women with local protection, but residence times of such agents are greatly reduced by the protective mucus layer, fluctuating hormone cycle, and complex anatomical structure of the reproductive tract. Polymeric nanoparticles (NPs) capable of encapsulating the desired cargo, penetrating through the mucosal surfaces, and delivering agents to the site of action have been explored. However, prolonged retention of polymer carriers and their enclosed materials may also be needed to ease adherence and confer longer-lasting protection against STDs. Here, we examined the fate of two poly(lactic acid)-hyperbranched polyglycerols (PLA-HPG) NP formulations – 1) nonadhesive PLA-HPG NPs (NNPs) and 2) surface-modified bioadhesive NPs (BNPs) – loaded with the antiretroviral elvitegravir (EVG) after intravaginal administration. BNP distribution was widespread throughout the reproductive tract, and retention was nearly 5 times higher than NNPs after 24h. Moreover, BNPs were found to be highly associated with submucosal leukocytes and epithelial cell populations for up to 48h after topical application, and EVG was retained significantly better in the vaginal lumen when delivered with BNPs as opposed to NNPs over a 24h period. Our results suggest that bioadhesive PLA-HPG NPs can greatly improve and prolong intravaginal delivery of agents, which may hold potential in providing sustained protection over longer durations.

[#]Correspondence should be addressed to W. Mark Saltzman: Department of Biomedical Engineering, Malone Engineering Center, Yale University, 55 Prospect Street, New Haven, CT 06511 USA. Tel: (203) 432-4262. E-mail: mark.saltzman@yale.edu.
[†]These authors contributed equally to this work

**Publisher's Disclaimer:** This is a PDF file of an unedited manuscript that has been accepted for publication. As a service to our customers we are providing this early version of the manuscript. The manuscript will undergo copyediting, typesetting, and review of the resulting proof before it is published in its final citable form. Please note that during the production process errors may be discovered which could affect the content, and all legal disclaimers that apply to the journal pertain.

**Conflict of Interest:** The authors declare no conflict of interest.

Author Manuscript Author Manuscript Author Manuscript Author Manuscript

**Keywords**

Intravaginal; Elvitegravir; Bioadhesive nanoparticles; Antiretroviral therapy; HIV prophylaxis; PLA-HPG

## 1. Introduction

Although decades of investigation has led to significant advancements in our understanding of how to treat and prevent human immunodeficiency virus (HIV), 2.1 million cases of newly acquired HIV infection worldwide occurred in 2015 [1]. Moreover, there are nearly 37 million individuals currently infected with HIV, and acquired immunodeficiency syndrome (AIDS) was responsible for 1 million deaths that same year [1]. The HIV epidemic remains at a staggeringly high level in African countries despite the development and optimization of many antiretroviral (ARV) therapies, microbicides, and protective barriers [2]. The persistence of HIV infection in the developing world may suggest the need for new approaches for prevention and treatment in order to dampen the severity of the epidemic, thereby reducing the aforementioned incidence rates of HIV and death rates attributed to AIDS.

The female reproductive tract serves as the site of entry for many bacterial and viral pathogens that can lead to sexually transmitted diseases (STDs). As such, intravaginal administration of therapeutics has long been a strategic approach for preventing and treating STDs such as HIV [3, 4]. Though intravaginal administration has certain advantages, such as minimal invasiveness and avoidance of first-pass metabolism [5], delivery of therapeutics in this manner can be challenging. Intravaginal delivery of drugs or other biological molecules must overcome the acidic pH and degradative enzymes of the vaginal environment [6, 7], the dense, protective layer of mucus that coats the vaginal epithelium [8], poor retention of non-viscous therapeutic formulations in the open-ended anatomical structure [9], and rapid biological changes in tissue and mucus properties correlating to hormonal cycles [10, 11].

In order to address barriers to successful microbicide delivery, vehicles must be designed to: 1) increase penetration into the rugae and epithelium to enhance microbicide protection and 2) prolong retention in the reproductive tract to reduce dosing and improve patient adherence, which has plagued many recent clinical trials assessing microbicide effectiveness [12]. Polymer nanoparticles (NPs) can overcome some of these concerns by providing protection for their encapsulated payload. Additionally, such particles can be designed for maximal, effective transport through the mucus barrier [13]. For example, the size and surface properties of particles can be modified to enhance penetration through the mucus barrier layer and increase penetration into the epithelium [14, 15]. However, NPs tend to be administered in non-viscous formulations, which can result in leakage and thus, shortened retention times [9]. For maximal effectiveness, drug containing NPs must remain in the lumen of the reproductive tract long enough to allow diffusion and penetration through the mucosal layer and subsequent association with the underlying cellular layers [8].

Poly(lactide-co-glycolide) (PLGA), a degradable polymer that has been used in many FDA approved devices, has long been the standard NP material for intravaginal delivery of

Author Manuscript Author Manuscript Author Manuscript Author Manuscript

therapeutics. PLGA NPs easily encapsulate a wide array of biological agents and can be engineered to provide appropriate release properties [16]. Polyethylene glycol (PEG) has been widely used as a surface addition to PLGA NPs to provide stability and enhanced mucosal penetration and delivery of therapeutic molecules in the treatment of cervicovaginal diseases [9, 17–21]. But recently it has been reported that immune responses can develop to PEG [22–24], which could be particularly harmful for repetitive delivery to a mucosal surface. Our group has recently developed a method for dramatically improving the stealth, aggregation-resisting, mucus-penetrating, and local retention properties of NPs, without the use of PEG. This new method involves the conjugation of poly(lactic acid) (PLA) to hyperbranched polyglycerols (HPG) to produce PLA-HPG NPs, with the HPG forming a corona on the NP surface (Figure 1A) [25]. Because this HPG layer should provide stealth properties to the NPs, HPG was directly compared to particles coated with PEG, which is the most widely used stealth material [26]. The NPs produced from PLA-HPG had a significantly longer half-life after intravenous injection, 10 hr, than NPs produced from PLA-PEG, 6 hr [25]. Because this stealth property is associated with a lack of adhesion to proteins and protein-rich surfaces, we call these PLA-HPG particles nonadhesive NPs or NNPs.

Furthermore, PLA-HPG NPs can be made bioadhesive. In these bioadhesive NPs (BNPs), the surface coating of the NNPs were oxidized by simple exposure to sodium periodate for brief periods; this procedure converts the vicinal diols on HPG to aldehydes [27]. Aldehydes on the BNPs are capable of forming stable Schiff base interactions with amine groups, such as N-terminal or lysine side chain of proteins [27, 28]. Our group has demonstrated that these BNPs, through amine interactions, can serve as an effective topical sunscreen through enhanced skin bioadhesion, which resists vigorous washing with water, thereby serving as a long-lasting potent UV protectant for the skin [27]. Additionally, we have recently reported the effectiveness of these BNPs in reducing systemic toxicity of the potent chemotherapeutic agent epothilone B (EB), enhancing retention of EB after intraperitoneal administration, and increasing therapeutic efficacy against the development of high-grade ovarian and endometrial carcinomas [28].

This current report describes the development and characterization of PLA-HPG NNP and BNP formulations (Figure 1A) encapsulating elvitegravir (EVG) (Figure 1B), a strand transfer inhibitor of HIV [29]. We explore whether these NP formulations can increase particle penetration and retention in the reproductive tissue, thereby prolonging the local dose and therapeutic efficacy of ARV prophylactic treatments against HIV. To test this hypothesis, we examine the distribution and retention of fluorescent NPs in the reproductive tracts after vaginal administration in mice. Specific nanoparticle-cell association was also explored to give insight into mucus penetration and tissue association as well as intravaginal EVG retention to assess long-term efficacy. In summary, we demonstrate that BNPs have significantly longer retention times after vaginal delivery than NNPs. The superior performance of BNPs makes sense: these nanoparticles can similarly penetrate mucus but once in contact with epithelial cells or leukocytes, they become immobilized and are retained for long periods. In contrast, the NNPs – lacking bioadhesive properties – are readily cleared by natural turnover of mucus or lymphatic drainage if they reach the tissue space (Figure 1C).

Author Manuscript Author Manuscript Author Manuscript Author Manuscript

## 2. Materials and methods

### 2.1. Materials

Elvitegravir was provided by Gilead Sciences (Foster City, CA) via CONRAD (Arlington, VA). PLA-HPG was synthesized as previously described [25]. IR-780 iodide, glycerol, $NaIO_4$, $Na_2SO_3$, bovine serum albumin (BSA), lactic acid, acetic acid, mucin, urea, glucose, Tween 80, Solutol (Kolliphor) HS 15, and HPLC-grade formic acid were obtained from Sigma-Aldrich. The 4-(4-(dihexadecylamino)styryl)-N-methylpyridinium iodide salt (DiA) and 4,6-diamidino-2 phenylindole (DAPI) stain were ordered from Invitrogen. Antibody stains anti-CD45 (ab10558) and anti-EpCAM (ab71916) and corresponding isotype controls for flow cytometry were purchased from Abcam. HPLC grade acetonitrile and water were purchased from VWR (J.T. Baker).

### 2.2. Nanoparticle preparation

To prepare NNPs, 100 mg of PLA-HPG was dissolved in 2.4 ml of ethyl acetate. For dye loaded particles, either IR-780 iodide dye or DIA (0.5 wt %) was dissolved in 0.6 ml of dimethyl sulfoxide (DMSO). For drug loaded particles, EVG (20% w/w) was dissolved in 0.6 ml of DMSO. The drug or dye solution was then combined with the polymer solution resulting in a polymer/dye or polymer/drug solvent mixture (ethyl acetate: DMSO = 4:1). The resulting solution was added to 4 ml deionized (DI) water under vortex and sonicated with a probe sonicator (4×, 10s each). Then, the emulsion was diluted in 20 ml of DI water and subsequently placed on a rotavapor for 30 min. The particle solution was washed by filtration using Amicon ultra-15 centrifugal filter units (100K cut-off) 3 times before being suspended in DI water. NNPs were flash frozen with liquid nitrogen and stored at −20°C until use [25, 27].

To convert NNPs into BNPs, NNPs were incubated with 0.1 M $NaIO_4$ and 10× phosphate buffered saline (PBS) (1:1:1 volume ratio) for 20 min. The reaction was quenched with 0.2 M $Na_2SO_3$ (1:3 volume ratio). BNPs were washed by filtration three times with DI water using Amicon ultra-0.5 ml filters (100K cutoff) and resuspended in DI water [27].

### 2.3. In *vitro* characterization of nanoparticles

The surface charge, diameter, and polydispersity index (PDI) of NP formulations (n=5) were determined by laser doppler electrophoresis and dynamic light scattering using a Zetasizer Nano ZS (Malvern Instruments). Particle morphologies were characterized by transmission electron microscopy (TEM) (FEI, Tecnai $G^2$ Spirit BioTWIN).

To determine the concentration of the IR-780 or DiA in dye loaded particle formulations, aqueous solutions of particles were diluted 10 fold in DMSO. The concentration of the IR-780 dye was quantified with a plate reader at absorbance of 650 nm. The concentration of DiA was quantified by fluorescence with a plate reader (em/ex 590/456 nm). Dye loading was calculated from a standard curve.

EVG loading in NP formulations was determined by high-performance liquid chromatography (HPLC) (Agilent 1100 HPLC) with ZORBAX Extend C18 analytical

Author Manuscript Author Manuscript Author Manuscript Author Manuscript

column (Agilent). NPs were diluted 10 fold in Acetonitrile and filtered with a 13mm HPLC syringe filter (Pall Laboratory, VWR). Acetonitrile/water supplemented with 0.1% formic acid was used as the mobile phase and the wavelength of the UV detector was set at 256 nm. Drug loading was determined from a standard curve.

In *vitro* drug release of NNPs and BNPs was determined by diluting a 100 μl suspension of EVG loaded NNPs or BNPs (n=3) 10 fold in a suspension of simulated vaginal fluid (SVF) (NaCl, 3.51 g/L; KOH, 1.40 g/L; $Ca(OH)_2$, 0.222 g/L; bovine serum albumin, 0.018 g/L; lactic acid, 2.00 g/L; acetic acid, 1.00 g/L; glycerol, 0.16 g/L; urea, 0.40 g/L; glucose, 5.0 g/L; mucin 1.5% w/v; pH 4.2) supplemented with 1% Tween 80 and 2% Solutol. The resulting solution was placed in microdialysis tubes (100 kDa cut-off) and floated in a 4L suspension of the same supplemented SVF. At each time point, microdialysis tubes (n=3) were removed, and the remaining EVG level in each tube was quantified using HPLC as described previously. At each time point the SVF solution in the large beaker was replaced with fresh buffer.

Similarly, to confirm dye molecules served as particle tracers, 100 μl of NNPs or BNPs loaded with IR-780 or DiA were placed microdialysis tubes (100 kDa cut-off). A similar protocol was carried out and the remaining dye at each time point was quantified with a plate reader as previously described.

To test the effect of NNPs and BNPs on cell viability, epithelial cell lines from the vagina (VK2/E6E7; ATCC CRL-2616) and cervix (End1/E6E7; ATCC CRL-2615) were cultured in Keratinocyte Serum Free (KSF) medium (GIBCO) supplemented with 0.1 ng/ml human recombinant EGF, 0.05 mg/ml bovine pituitary extract, and 1% penicillin/streptomycin. Vaginal epithelial cells (VEC) and cervical epithelial cells (CEC) in 180 μL of KSF medium were plated in each well of a 96-well plate at a density of 2,000 per well and maintained at 37 °C to incubate overnight. The following day, 20 μL of either KSF medium, blank NNPs, blank BNPs, EVG/NNPs, EVG/BNPs was added to cells. Cells were incubated at 37 °C for 72 h, and then cell viability was quantified with a Cell Titer Blue Assay (Thermo Fisher Scientific).

### 2.4. Animal Preparation

All procedures and experiments were approved by the Yale University Institutional Animal Care and Use Committee. Five days prior to NP delivery, C57BL/6 mice (6–8 weeks old, Charles River Laboratories) were treated with Depo-Provera (Pfizer) by subcutaneous injection (2 mg/animal) to synchronize mice into the diestrus phase. To ensure reproducibility, mice were lavaged 24h prior to experimentation and only those confirmed to be in the diestrus phase were used for experimentation.

### 2.5. In *vivo* toxicity of nanoparticles

Fifteen μL of either PBS (control), EVG/NNPs, or EVG/BNPs were administered intravaginally to mice (n=3 PBS, n=5 EVG/NNPs, n=5 EVG/BNPs). After 24h, mice were sacrificed and vaginal tissue was harvested for histological examination. Samples were fixed overnight in 10% neutral buffered formalin and sent to the histology service core at the Yale School of Medicine (Section of Comparative Medicine) for paraffin embedding and

Author Manuscript Author Manuscript Author Manuscript Author Manuscript

hematoxylin and eosin (H&E) staining. Representative H&E stained tissue sections were examined by a pathologist blinded to the experimental groups using an Olympus BX45 microscope. Tissue sections were analyzed for toxicity based on epithelial disruption, epithelial layer number, leukocyte infiltration, apoptotic cells, and cellular debris in the lumen. Images were collected using an Olympus BX61 microscope with a SPOT Flex 64 MP digital color camera.

### 2.6 Nanoparticle retention and distribution in vaginal lumen

Ten μL of either IR-780/NNPs or IR-780/BNPs were administrated intravaginally to mice (n=5). At each time point, mice were sacrificed and vaginal tissue was harvested for ex *vivo* imaging. Particle retention and distribution was visualized and quantified using a live imaging instrument (In-Vivo MS FX PRO, Bruker). Positive signals were determined in reference to untreated control tissues and quantified using the instrument software. The lower end of the fluorescence intensity range was adjusted to eliminate any tissue auto-fluorescence from untreated controls and the higher end of the fluorescence intensity range was set to avoid saturation of fluorescence.

To further assess particle distribution and retention of BNPs, mice (n=3) were treated with 10 μL of DiA/BNPs. Mice were sacrificed at 24h after treatment and vaginal tissue was excised. Harvested tissues were embedded in OCT medium and flash frozen with liquid nitrogen. Samples were sliced using a cryostat (Leica CM 3050S) to represent representative transverse sections throughout the reproductive tract. Sectioning began from the uterine horn end to the vaginal opening end using 10 μm tissue section to approximate single cell layer thickness. Sectioned tissue samples were stained with DAPI and microscopically imaged (SteREO Lumar V.12, Zeiss). Positive BNP signals were determined using ImageJ and were in reference to untreated control tissue samples.

### 2.7. Nanoparticle-cell association

Fluorescent activated cell sorting (FACS) was used to assess particle-cell associations and cell-specific particle distribution. Mice (n=5) were intravaginally administered with 15 μL of either DiA loaded NNPs or BNPs. At each time point, mice were sacrificed and vaginal tissue was excised. The tissue was cut into several pieces, incubated in 2 mL of 0.4% collagenase for 30 min, homogenized manually, and then filtered using a 70 μm strainer. The resulting single cell suspension was pelleted and resuspended in 2% BSA. The cells were then incubated with anti-CD45 antibody and anti-EpCAM for 10 min. After staining, cells were washed with 2% BSA 3 times for 10 min each. Cells were resuspended in 250 μl of 2% BSA and samples were sent for FACS (Attune N×T, Invitrogen). Positive fluorescent antibody signals in each sample were ensured with comparison to corresponding isotype antibody controls and appropriate gates were set using control cell populations not treated with NNPs or BNPs.

### 2.8. Retention profile of EVG in reproductive tissue

Fifteen μL of a PBS/EVG, NNP/EVG or BNP/EVG suspension was delivered intravaginally. At each time point, mice (n=5) were sacrificed and vaginal tissue was excised. Tissues were homogenized in 0.7 mL of DMSO. After homogenization, samples were centrifuged at

Author Manuscript Author Manuscript Author Manuscript Author Manuscript

10,000 rpm for 10 min and the supernatant was collected and evaporated with a Speedvac. Samples were then reconstituted in 0.5 mL of acetonitrile and filtered, as previously described. EVG in the processed tissue samples was quantified using HPLC as previously described.

### 2.9. Data Analysis

All graphs were prepared using GraphPad Prism software. Flow cytometry data were analyzed using FlowJo software (TreeStar). Error bars represent either standard deviation or standard error of the mean (SEM) and have been indicated appropriately in each figure caption. Statistical significance was calculated using a two-tailed unpaired nonparametric Mann Whitney U test ($\alpha = 0.05$) with GraphPad Prism software. Significance is represented on plots as ns > 0.05, *< 0.05, ** < 0.01.

## 3. Results

### 3.1. NP synthesis and characterization

PLA-HPG nanoparticles encapsulating EVG were synthesized using a single emulsion protocol. The optimal formulation, based on NNP size and EVG encapsulation efficiency, was found to require preparation by nanoemulsion, an initial PLA-HPG concentration of 100 mg/ml and 20% (w/w) of EVG (Table s1). The size of EVG/NNPs was <150 nm, which remained similar even after conversion to EVG/BNPs with $NaIO_4$ treatment. The polydispersity index of EVG/NNPs and EVG/BNPs was low (Figure 2A). This result was confirmed by TEM, which also demonstrated NNP/EVG and BNP/EVG morphology was spherical and fairly uniform in size. (Figure 2B–C).

To confirm that EVG loaded nanoparticles had the potential to provide an extended, controlled release of EVG, EVG/NNPs and EVG/BNPs were places in dialysis tubes (100 kDa cut-off) and dialyzed in SVF. Both NNPs and BNPs had a similar EVG release profile (Figure 2D). After an initial burst release of EVG (~40%) within the first 8h, both NNPs and BNPs demonstrated a slower and more stable release up to 3d in the SVF. The release rate of EVG from both NNPs and BNPs was greatly reduced after 3d such that from day 3 to day 4 the release was ~5 ng EVG/mg NP/day.

### 3.2 NPs do not cause toxicity in *vitro* or in *vivo*

To test NP toxicity, in *vitro* cultured human VEC and CEC lines were treated with EVG/NNPs and EVG/BNPs at varying concentrations, and after incubating for 72h, cells were assessed for viability. The addition of NNPs and BNPs did not decrease cell viability relative to untreated controls in both VEC (Figure 2E) and CEC lines (Figure 2F) at all concentrations tested, ranging from 100 ng/ml to 100 mg/ml. Additionally, in *vivo* toxicity of EVG/NNPs and EVG/BNPs was analyzed using H&E stained sections of treated tissue. PBS-treated tissue was used as control. Tissues exposed to either NNP or BNP formulations appeared similar to control tissues, and, based on the assessment of an expert pathologist, there was no evidence of toxicity or inflammation in any group, as assessed by epithelial disruption and damage, epithelial cell layer number, cellular content in the lumen, leukocyte infiltration and visible apoptotic cells (Figure 3).

Author Manuscript Author Manuscript Author Manuscript Author Manuscript

### 3.3. BNPs enhance retention and distribution of nanoparticles in the vaginal lumen

To test whether BNPs provide prolonged retention in vaginal tissue as compared to NNPs, IR-780 dye loaded NNPs and BNPs were delivered intravaginally and the remaining dye percentage was quantified after 12h and 24h. IR-780/NNPs and IR-780/BNPs had comparable diameters and morphology to EVG/NNPs and EVG/BNPs, respectively (Figure 2A–C and s1A–B). Furthermore, little IR-780 dye was released from NNPs and BNPs over 48h when incubated in SVF, with ~90% of dye remaining in both NNPs and BNPs even after 48h (Figure s2A). Visually, BNPs demonstrated enhanced retention and distribution throughout the vaginal lumen 12h and 24h after particle administration (Figure 4A). BNPs had ~70% retention 12h post treatment, which was over two-fold higher compared to NNPs. BNPs had ~40% particle retention at 24h post treatment, nearly four-fold higher than NNPs (Figure 4B). These differences were found to be highly significant.

To further assess BNP retention and distribution at 24h, mice were similarly treated with DiA/BNPs. Like IR-780/BNPs and IR-780/NNPs (Figure s1A–B), DiA/BNPs and DiA NNPs (Figure s1C–D) exhibited similar morphology to EVG/BNPs and EVG/NNPs (Figure 2B–C), and had over 90% dye retention even up to 96h of incubation in SVF (Figure s2B). At 24h, tissue was harvested, cut into transverse sections, stained with DAPI and imaged for fluorescence. Representative sections of the vaginal tissue showed widespread distribution of BNPs lining the vaginal epithelium and rugae at 24h (Figure 4C).

### 3.4. BNPs improve nanoparticle-cell interaction in vaginal cell populations

BNPs demonstrated excellent retention and distribution across the vaginal surfaces, so we next wanted to determine whether BNPs were capable of providing enhanced association with relevant cell population in the vaginal tract. Treated and harvested vaginal tissues were homogenized into a single cell suspension for FACS. Leukocytes were gated on $CD45^+$ $EpCAM^-$ and were found to represent ~27% of the overall cell population (Figure 5A). Epithelial cells were gated on $CD45^-$ $EpCAM^+$ and represented over 13% of the total cell population (Figure 5B). At 24h, NNP treated mice had an increase in DiA expression in both $CD45^+$ and $EpCAM^+$ cell populations compared to untreated controls (Figure 5C), and this trend was even further pronounced in BNP treated mice (Figure 5D). Similar trends indicating increased DiA association cell populations of BNP treated mice compared to both NNP treated and untreated mice were observed between 12h and 48h in $CD45^+$ cells and between 12h and 72h in $EpCAM^+$ cells (Figure s3). The difference in the percentage of cells that were $CD45^+$ $DiA^+$ and $EpCAM^+$ $DiA^+$ between NNP and BNP treated mice was found to be statistically significant at 12h, 24h, 48h, and 72h for $CD45^+$ cell populations (Figure 5E) and 12h, 24h, and 48h for $EpCAM^+$ cell populations (Figure 5F).

The mean fluorescence intensity (MFI) of $CD45^+$ $DiA^+$ and $EpCAM^+$ $DiA^+$ were not significantly different between NNP and BNP treated mice at 12h (Figure 5G–H). However, MFI for BNP treated mice was significantly higher than for NNP treated mice at 24h in the $EpCAM^+$ $DiA^+$ population (Figure 5H). The $CD45^+$ $DiA^+$ cell population presented an increase in MFI of BNP treated mice relative to those treated with NNP at 24h, but this was not statistically significant (Figure 5G). The most significant increase in MFI between NNP and BNP treated mice for both $CD45^+$ $DiA^+$ and $EpCAM^+$ $DiA^+$ populations was observed

Author Manuscript Author Manuscript Author Manuscript Author Manuscript

at 48h. In $CD45^+$ $DiA^+$ cells, the MFI remains significantly increased in BNP treated mice relative to NNP treated mice at 72h, but this significance is not observed in $EpCAM^+$ $DiA^+$ cells (Figure 5G–H).

### 3.5. BNPs prolong EVG retention after intravaginal administration

After observing that BNPs are retained longer than NNPs after intravaginal administration and that BNPs are more readily associated with and internalized by vaginal cell populations, we next wanted to determine whether EVG delivered by BNPs would have prolonged retention in the vaginal tract. EVG delivered by BNPs (EVG/BNPs) was compared to EVG delivered by NNPs (EVG/NNPs) or without any encapsulant (free EVG). At 4h post-treatment, the EVG/BNP group retained 90% of the initial dose while the EVG/NNPs and free EVG groups retained 80% and 75% of the initial dose, respectively (Figure 6). EVG/BNPs had a statistically significant increase in retention over free EVG but not EVG/NNPs at this time point. At 8h post treatment, the EVG/BNPs, EVG/NNPs and free EVG groups retained 80%, 40% and 30% of the initial EVG dose, respectively, with the EVG/BNP group having very significant increases in retention as compared to the other two groups (Figure 6). No statistical difference was observed between EVG/NNPs and free EVG. A similar trend and significance levels were observed at 12h with the EVG/BNP group still maintain 60% of the initial EVG dose (Figure 6).

At 18h, the EVG/NNP group retained 10% of the initial dose, which was significantly higher than free EVG (less than 5% of the initial EVG amount). The EVG/BNP groups had nearly 20% retention, which was very statistically significant compared to the EVG/NNP and free EVG treated groups at 18h (Figure 6). At 24h post treatment, EVG/BNPs retained 10% of the initial dose, which was statistically different than the free EVG (<1%) and EVG/NNP (<2%) groups.

## 4. Discussion

One of the main challenges hindering the effectiveness of vaginal microbicides use is drug retention in the vaginal lumen [9]. PEG-modified PLGA particle formulations have notably achieved good initial distribution throughout the vaginal lumen, including rugae [9, 21, 30]. However, prolonged retention in the reproductive tract beyond several hours has not been widely explored. Here, we report the development of a potentially long-acting bioadhesive nanoparticle capable of extended drug release and retention over multiple days. EVG/NNPs and EVG/BNPs formed virus sized particles (<150 nm) and were optimized to provide a controlled release profile in *vitro*. Though an imperfect representation of the vaginal microenvironment, SVF was used to simulate NP exposure to the vaginal fluids; the NP formulation maintained stability and released EVG slowly over a 4d period (Figure 2C). The release curves of all EVG/NNPs and EVG/BNPs were similar to what we have seen in our previous studies using PLA-HPG formulated particles [25, 28]. Together, these data suggest that our NP formulations are small enough to be internalized by cells yet stable enough to provide a controlled release profile over an extended period of time.

Based on our previous work with PLA-HPG BNPs [27, 28], we hypothesized that the conversion of vicinal diols (NNPs) to aldehydes (BNPs) will result in Schiff-base

Author Manuscript Author Manuscript Author Manuscript Author Manuscript

interactions with the vaginal epithelium, thereby preventing BNP clearance through mucosal turnover. To test this hypothesis, IR-780 or DiA dye loaded NNPs and BNPs were used as tracers, which had similar size to EVG/NNPs and EVG/BNPs as well as substantial dye retention (90%) over multiple days in SVF (Figure 2A, Figure s2). These data suggest that dye loaded particles are useful markers for NP distribution. Dye loaded BNPs showed significantly enhanced particle retention at both 12h and 24h compared to conventional mucus-penetrating particles, such as NNPs (Figure 4A–B). Likewise, BNP retention seen at 24h was superior to other mucus-penetrating PLGA NPs used topically [9, 21]. Vaginal rugae have been notably difficult for therapeutics to penetrate [31], hindering the effectiveness of many NP carriers. However, distribution of BNPs throughout the vaginal epithelium surface was very dense and widespread throughout the rugae even up to 24h after topical administration (Figure 4C), which may confer prolonged therapeutic effects against STDs.

To determine the safety of EVG/NNPs and EVG/BNPs for topical use, we tested for their toxicity in *vitro* and in *vivo*. NNP and BNP formulations showed no toxicity to VEC and CEC lines even when cultured at very high doses (Figure 2E–F). Safety of NNPs and BNPs was further tested after intravaginal administration. H&E staining of tissues revealed no evidence of inflammation, irritation, or damage to the reproductive tissue after topical application of NPs. These results were in line with our previous findings, which have shown that NPs produced from PLA-HPG showed no toxicity when exposed at high doses to cultured cells and tissues. For example, similar to the results reported here, high doses of NNPs and BNPs previously showed no toxicity in multiple cell lines, including Lewis lung carcinoma, uterine serous carcinoma, Hela, human umbilical vein endothelium, A549, B16, Chinese hamster ovary, human embryonic kidney 293T, KB, and LNCaP. Moreover, repeated intraperitoneal injection of BNPs (5 mg) once a week for 5 weeks showed no systemic toxic effects, such as behavioral changes or weight loss [25, 28]. Also, we previously demonstrated that repeated topical application of BNPs to the skin in *vivo* showed no toxicity, inflammation, or cutaneous irritancy [27].

Though low molecular weight aldehydes are known to have toxicity risks [32], the low toxicity of BNPs is thought to be a result of several factors. Despite aldehyde groups covering the BNP surface, the covalent linkage of these surface aldehydes to BNPs limits their distribution. Additionally, aldehydes are common in many foods and metabolites, which may confer high tolerance, and aldehyde groups can be readily detoxified by aldehyde dehydrogenase [33].

EVG falls into a class of antiretrovirals that function as integrase inhibitors [29]. EVG specifically acts against HIV-1 via strand transfer inhibition, thereby preventing translocation of the reverse transcribed viral DNA into the nucleus and subsequent integration into the genome. As such, the mechanism of action requires that EVG be internalized by the cell types in which HIV-1 infects and uses to replicate. Using fluorescent NPs, we observed widespread particle coverage in the vaginal tissue (Figure 4C). As such, we sought to determine whether particles were associating with leukocyte cell populations that HIV-1 targets for infection and replication. $CD4^+$ T cells, a subset of $CD45^+$ leukocytes, serve as the primary targets for HIV-1 infection and replication [34, 35]. In addition, we

Author Manuscript Author Manuscript Author Manuscript Author Manuscript

sought to determine whether BNPs also associated with cervical epithelial cells expressing the adhesion molecule EpCAM, which are not known to play a role in HIV-1 replication but do play a role in the infection and replication of herpes simplex virus (HSV) [35].

Interestingly, FACS resulted indicated at least some fraction of $CD45^+$ and $EpCAM^+$ cell populations were associated with BNPs for up to 72h in *vivo*. Also, significant increases in BNP association over that of NNPs was observed in $CD45^+$ cells for up to 72h and $EpCAM^+$ cells for up to 48h. The sizeable increase in the percentage of $DiA^+$ $CD45^+$ and $DiA^+$ $EpCAM^+$ cells between 12h and 24h of BNP treated mice was thought to be a result of particle-cell association versus particle internalization. Because BNPs stick to the cell surface through Schiff-base interactions, our thought was that the BNPs would more likely to be internalized due to prolonged interactions. During the rather vigorous homogenization and wash steps for FACS preparation, we believe that most particles on the cell surface are removed. As such, only those cell with internalized particles will be $DiA^+$. Decreases in the percent of $DiA^+$ cells at 48h and 72h were expected, as the epithelial cell layers divide and shed while some leukocytes likely undergo apoptosis and others are recruited to the vaginal lumen and tissue [36]. The initial similarity in MFI between the two groups seems to indicate that initial association and internalization of particles are similar. However, as NNPs are shed through mucosal secretions, which can be up to 1 mL/day for mice in diestrus [8], the MFI reduces as early as 24h but even more so at 48h. The MFI drops off more slowly in cell populations treated with BNPs, which is in line with our initial hypothesis that BNPs are retained longer through protein interactions and thus avoid the same fate as NNPs.

The cellular association between BNPs and both leukocyte and epithelial cell populations indicate the potential usefulness of BNPs to co-deliver microbicides against multiple STDs. For example, HSV-2 infection has been linked to an increased risk of HIV-1 infection due to damaged cervical epithelium caused by HSV-2 infection [37, 38]. Antiretroviral therapy has been effective in HIV treatment and prevention, while topical application of mucus-penetrating PLGA NPs loaded with acyclovir have shown promise in preventing HSV-2 acquisition after intravaginal challenge in mice [21]. Likewise, recent studies using PLGA-based NPs loaded with siRNA have shown potential for the prevention and treatment of STDs in mice, including HSV-2 [18, 19]. Thus, our BNPs may provide a carrier in which multiple therapeutic or prophylactic agents can be simultaneously encapsulated and delivered to relevant cervicovaginal cell populations to prevent the acquisition of concomitant STDs, such as HIV-1 and HSV-2.

EVG delivered as free EVG or EVG/NNPs had similar retention profiles over the course of 24h (Figure 6, insert). EVG/NNPs did have significant increases in EVG retention at 18h and 24h compared to free EVG, but the overall trend for EVG elimination from the vaginal tissue and lumen appeared to be comparable. However, the EVG retention profile of mice treated with EVG/BNPs was strikingly different between 0h and 18h (Figure 6, insert), indicating that bioadhesive modification may play a vital role in preventing rapid elimination of EVG, and perhaps other therapeutic molecules, from the reproductive tract.

Author Manuscript Author Manuscript Author Manuscript Author Manuscript

## 5. Conclusion

Our understanding of HIV has increased substantially over the past several decades, and many new agents are available for treatment and prevention of HIV infections. Still, there remains a need for longer lasting and more easily adherent treatment regimens in order to quell the HIV/AIDS epidemic. Topical application of therapeutic molecules to the reproductive tract, which serves as the primary infection site for many STDs, has been widely explored, but prolonged usefulness of these agents has been hindered by the complex physiological and anatomical barriers in the vaginal lumen. We report here that polymeric NPs made of PLA-HPG can overcome these challenges by effectively encapsulating and delivering a potent antiretroviral, EVG. The surface of these NPs can be modified to yield a bioadhesive coating to overcome limitations in NP/therapeutic molecule retention. Our results show that PLA-HPG BNPs are retained along the vaginal epithelium longer than PLA-HPG NNPs and other PLGA-based mucus-penetrating particles. Furthermore, BNPs were highly associated with epithelial and leukocyte populations in the reproductive tract for multiple days, and EVG retention was prolonged with BNP delivery as compared to delivery with NNP or free drug groups. These BNPs may be more effective for prolonged delivery of individual agents, or perhaps even multiple microbicides in combination, that require cellular internalization to take effect, such as antivirals, siRNA, and plasmid DNA. Our study demonstrates the potential for a bioadhesive polymeric nanoparticle platform with enhanced retention capabilities, providing promise for improved intravaginal therapeutic delivery.

## Supplementary Material

Refer to Web version on PubMed Central for supplementary material.

## Acknowledgments

The authors thank Terrence Wu and Yuhang Jiang for technical assistance with HPLC and TEM, respectively. We also thank Ganesh Cherala for helpful discussions. This work is made possible by the generous support of the American people through the United States Agency for International Development (USAID) under an agreement (MAPS2-15-045) under a Cooperative Agreement (AID-OAA-A-14-00010) to CONRAD, Department of Obstetrics and Gynecology, Eastern Virginia Medical School. Partial support to WM Saltzman was provided by a grant from the US National Institutes of Health (NIH EB00487), partial support to Muneeb Mohideen was provided by the National Institute of Diabetes and Digestive and Kidney Diseases of the National Institutes of Health (T35DK104689), and partial support to Elias Quijano was provided by the National Institutes of Health Medical Scientist Program Training Grant (T32GM007205). The views expressed by the authors do not necessarily reflect the views of USAID, the National Institutes of Health, the United States Government, or CONRAD.

## References

1. WHO. Global Summary of the AIDS Epidemic. Vol. 2015. World Health Organization; 2015.
2. Morgan D, Whitworth JAG. The natural history of HIV-1 infection in Africa. Nat Med. 2001; 7:143–5. [PubMed: 11175832]
3. Wilson DP, Coplan PM, Wainberg MA, Blower SM. The paradoxical effects of using antiretroviral-based microbicides to control HIV epidemics. Proc Natl Acad Sci U S A. 2008; 105:9835–40. [PubMed: 18606986]
4. Grant RM, Hamer D, Hope T, Johnston R, Lange J, Lederman MM, et al. Whither or wither microbicides? Science. 2008; 321:532–4. [PubMed: 18653884]

Author Manuscript Author Manuscript Author Manuscript Author Manuscript


5. Hussain A, Ahsan F. The vagina as a route for systemic drug delivery. J Control Release. 2005; 103:301–13. [PubMed: 15763615]
6. Lee VH. Enzymatic barriers to peptide and protein absorption. Crit Rev Ther Drug Carrier Syst. 1988; 5:69–97. [PubMed: 3052875]
7. Woolfson AD, Malcolm RK, Gallagher R. Drug delivery by the intravaginal route. Crit Rev Ther Drug Carrier Syst. 2000; 17:509–55. [PubMed: 11108158]
8. Cone RA. Barrier properties of mucus. Adv Drug Deliv Rev. 2009; 61:75–85. [PubMed: 19135107]
9. Cu Y, Booth CJ, Saltzman WM. In vivo distribution of surface-modified PLGA nanoparticles following intravaginal delivery. J Control Release. 2011; 156:258–64. [PubMed: 21763739]
10. Wira CR, Fahey JV, Ghosh M, Patel MV, Hickey DK, Ochiel DO. Sex hormone regulation of innate immunity in the female reproductive tract: the role of epithelial cells in balancing reproductive potential with protection against sexually transmitted pathogens. Am J Reprod Immunol. 2010; 63:544–65. [PubMed: 20367623]
11. Wira CR, Patel MV, Ghosh M, Mukura L, Fahey JV. Innate immunity in the human female reproductive tract: endocrine regulation of endogenous antimicrobial protection against HIV and other sexually transmitted infections. Am J Reprod Immunol. 2011; 65:196–211. [PubMed: 21294805]
12. Friend DR, Kiser PF. Assessment of topical microbicides to prevent HIV-1 transmission: concepts, testing, lessons learned. Antiviral Res. 2013; 99:391–400. [PubMed: 23845918]
13. Cu Y, Saltzman WM. Controlled surface modification with poly(ethylene)glycol enhances diffusion of PLGA nanoparticles in human cervical mucus. Mol Pharm. 2009; 6:173–81. [PubMed: 19053536]
14. Mestecky J, Moldoveanu Z, Russell MW. Immunologic uniqueness of the genital tract: challenge for vaccine development. Am J Reprod Immunol. 2005; 53:208–14. [PubMed: 15833098]
15. Vila A, Gill H, McCallion O, Alonso MJ. Transport of PLA-PEG particles across the nasal mucosa: effect of particle size and PEG coating density. J Control Release. 2004; 98:231–44. [PubMed: 15262415]
16. Mundargi RC, Babu VR, Rangaswamy V, Patel P, Aminabhavi TM. Nano/micro technologies for delivering macromolecular therapeutics using poly(D,L-lactide-co-glycolide) and its derivatives. J Control Release. 2008; 125:193–209. [PubMed: 18083265]
17. Blum JS, Weller CE, Booth CJ, Babar IA, Liang X, Slack FJ, et al. Prevention of K-Ras- and Pten-mediated intravaginal tumors by treatment with camptothecin-loaded PLGA nanoparticles. Drug Deliv Transl Res. 2011; 1:383–94. [PubMed: 25419505]
18. Woodrow KA, Cu Y, Booth CJ, Saucier-Sawyer JK, Wood MJ, Saltzman WM. Intravaginal gene silencing using biodegradable polymer nanoparticles densely loaded with small-interfering RNA. Nat Mater. 2009; 8:526–33. [PubMed: 19404239]
19. Steinbach JM, Weller CE, Booth CJ, Saltzman WM. Polymer nanoparticles encapsulating siRNA for treatment of HSV-2 genital infection. J Control Release. 2012; 162:102–10. [PubMed: 22705461]
20. Yang M, Yu T, Wang YY, Lai SK, Zeng Q, Miao B, et al. Vaginal delivery of paclitaxel via nanoparticles with non-mucoadhesive surfaces suppresses cervical tumor growth. Adv Healthc Mater. 2014; 3:1044–52. [PubMed: 24339398]
21. Ensign LM, Tang BC, Wang YY, Tse TA, Hoen T, Cone R, et al. Mucus-penetrating nanoparticles for vaginal drug delivery protect against herpes simplex virus. Sci Transl Med. 2012; 4:138ra79.
22. Yang Q, Lai SK. Anti-PEG immunity: emergence, characteristics, and unaddressed questions. Wiley Interdiscip Rev Nanomed Nanobiotechnol. 2015; 7:655–77. [PubMed: 25707913]
23. Verhoef JJF, Anchordoquy TJ. Questioning the use of PEGylation for drug delivery. Drug Deliv Transl Re. 2013; 3:499–503.
24. Mima Y, Hashimoto Y, Shimizu T, Kiwada H, Ishida T. Anti-PEG IgM Is a Major Contributor to the Accelerated Blood Clearance of Polyethylene Glycol-Conjugated Protein. Mol Pharmaceut. 2015; 12:2429–35.
25. Deng Y, Saucier-Sawyer JK, Hoimes CJ, Zhang J, Seo YE, Andrejecsk JW, et al. The effect of hyperbranched polyglycerol coatings on drug delivery using degradable polymer nanoparticles. Biomaterials. 2014; 35:6595–602. [PubMed: 24816286]

Author Manuscript Author Manuscript Author Manuscript Author Manuscript


26. Hrkach J, Von Hoff D, Mukkaram Ali M, Andrianova E, Auer J, Campbell T, et al. Preclinical development and clinical translation of a PSMA-targeted docetaxel nanoparticle with a differentiated pharmacological profile. Sci Transl Med. 2012; 4:128ra39.
27. Deng Y, Ediriwickrema A, Yang F, Lewis J, Girardi M, Saltzman WM. A sunblock based on bioadhesive nanoparticles. Nat Mater. 2015; 14:1278–85. [PubMed: 26413985]
28. Deng Y, Yang F, Cocco E, Song E, Zhang J, Cui J, et al. Improved i.p. drug delivery with bioadhesive nanoparticles. Proc Natl Acad Sci U S A. 2016; 113:11453–8. [PubMed: 27663731]
29. Lampiris HW. Elvitegravir: a once-daily, boosted, HIV-1 integrase inhibitor. Expert Rev Anti Infect Ther. 2012; 10:13–20. [PubMed: 22149610]
30. Ensign LM, Hoen TE, Maisel K, Cone RA, Hanes JS. Enhanced vaginal drug delivery through the use of hypotonic formulations that induce fluid uptake. Biomaterials. 2013; 34:6922–9. [PubMed: 23769419]
31. Alexander NJ, Baker E, Kaptein M, Karck U, Miller L, Zampaglione E. Why consider vaginal drug administration? Fertil Steril. 2004; 82:1–12. [PubMed: 15236978]
32. O'Brien PJ, Siraki AG, Shangari N. Aldehyde sources, metabolism, molecular toxicity mechanisms, and possible effects on human health. Crit Rev Toxicol. 2005; 35:609–62. [PubMed: 16417045]
33. Vasiliou V, Thompson DC, Smith C, Fujita M, Chen Y. Aldehyde dehydrogenases: from eye crystallins to metabolic disease and cancer stem cells. Chem Biol Interact. 2013; 202:2–10. [PubMed: 23159885]
34. Bour S, Geleziunas R, Wainberg MA. The human immunodeficiency virus type 1 (HIV-1) CD4 receptor and its central role in promotion of HIV-1 infection. Microbiol Rev. 1995; 59:63–93. [PubMed: 7708013]
35. Bomsel M, Alfsen A. Entry of viruses through the epithelial barrier: pathogenic trickery. Nat Rev Mol Cell Biol. 2003; 4:57–68. [PubMed: 12511869]
36. Ensign LM, Cone R, Hanes J. Nanoparticle-based drug delivery to the vagina: a review. J Control Release. 2014; 190:500–14. [PubMed: 24830303]
37. Huang W, Hu K, Luo S, Zhang M, Li C, Jin W, et al. Herpes simplex virus type 2 infection of human epithelial cells induces CXCL9 expression and CD4+ T cell migration via activation of p38-CCAAT/enhancer-binding protein-beta pathway. J Immunol. 2012; 188:6247–57. [PubMed: 22586042]
38. Horbul JE, Schmechel SC, Miller BR, Rice SA, Southern PJ. Herpes simplex virus-induced epithelial damage and susceptibility to human immunodeficiency virus type 1 infection in human cervical organ culture. PLoS One. 2011; 6:e22638. [PubMed: 21818356]

Author Manuscript Author Manuscript Author Manuscript Author Manuscript

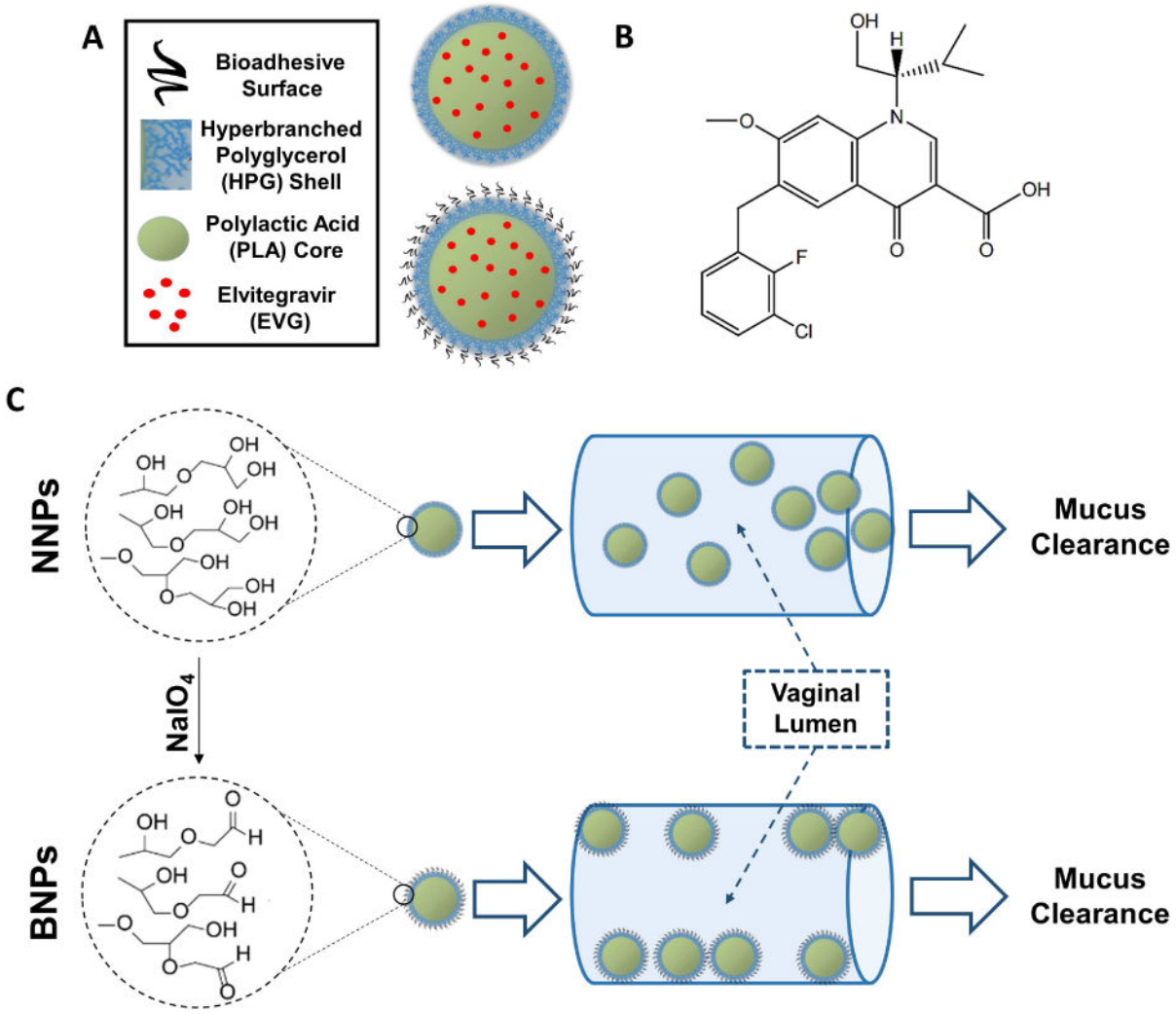


**Figure 1. Nanoparticle design and fate**

A) NNPs (top) and BNPs (bottom) are comprised of a hydrophobic interior (PLA and EVG) and hydrophilic exterior (HPG). BNPs have an additional bioadhesive coating on the particle surface produced by conversion of vicinal diols on NNPs to aldehydes on BNPs. B) Molecular structure of EVG. C) Schematic showing the conversion of NNPs to BNPs by $NaIO_4$ and hypothesized fate of each of the nanoparticles after intravaginal administration. NNPs are cleared away during normal vaginal secretions and mucus clearance. BNPs adhere to the epithelial surface, thereby avoiding rapid elimination.

Author Manuscript Author Manuscript Author Manuscript Author Manuscript

A

| Nanoparticle Formulation | Diameter (nm) | PDI |
|---|---|---|
| NNPs | 102 ± 4 | 0.23 ± 0.02 |
| BNPs | 98 ± 7 | 0.24 ± 0.03 |
| DiA/NNPs | 118 ± 5 | 0.22 ± 0.01 |
| DiA/BNPs | 118 ± 2 | 0.20 ± 0.02 |
| IR-780/NNPs | 129 ± 6 | 0.19 ± 0.04 |
| IR-780/BNPs | 127 ± 4 | 0.19 ± 0.02 |
| EVG/NNPs | 135 ± 3 | 0.27 ± 0.02 |
| EVG/BNPs | 131 ± 5 | 0.25 ± 0.03 |

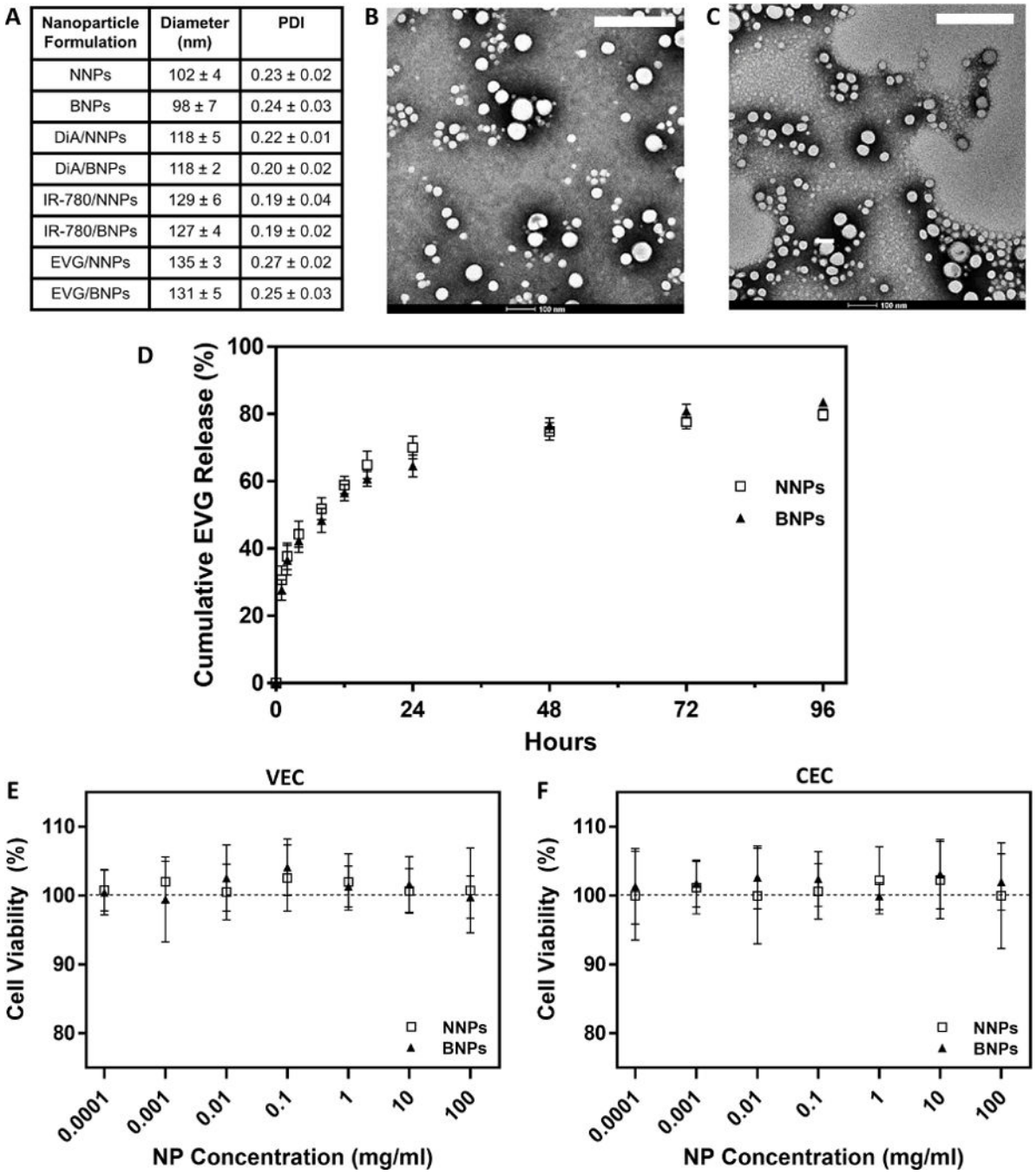


**Figure 2. In *vitro* nanoparticle characterization**

A) Hydrodynamic diameters and polydispersity index of nanoparticle formulations. Data is shown as mean ± SD (n=5). TEM images of B) EVG/NNPs and C) EVG/BNPs. Scale bar on images represents 200 nm. D) In *vitro* release profile of EVG/NNPs and EVG/BNPs in a simulated vaginal fluid. Data is shown as mean ± SD (n=3). Cell viability of cultured human E) vaginal epithelial cells (VEC) and F) cervical epithelial cells (CEC) treated with EVG/NNPs and EVG/BNPs in *vitro*. Data is shown as mean ± SD (n=8).

Author Manuscript Author Manuscript Author Manuscript Author Manuscript

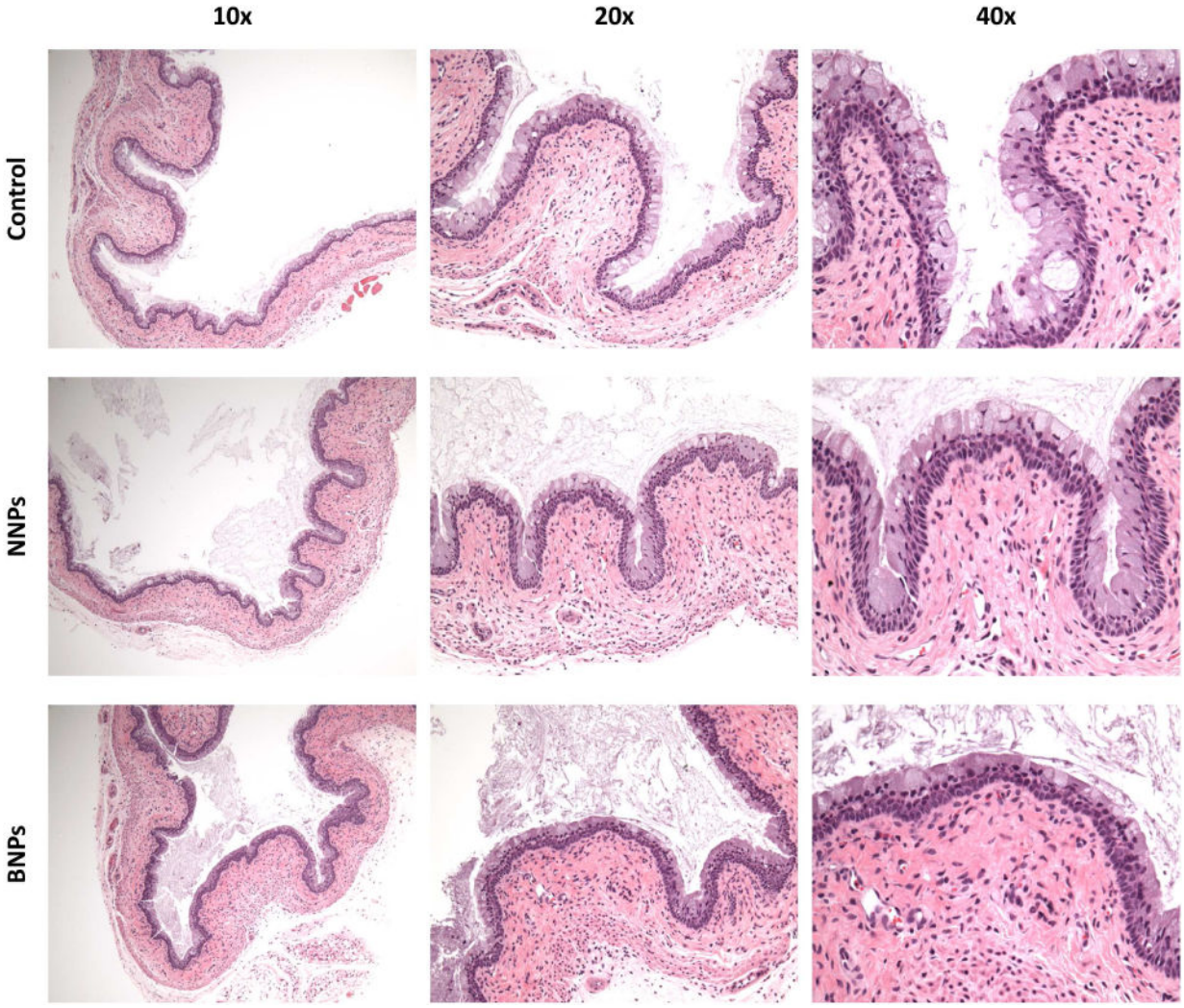


**Figure 3. In *vivo* toxicity evaluation of NP treated reproductive tracts**

H&E sections of tissues treated with PBS as a control (top row), EVG/NNPs (middle row) and EVG/BNPs (bottom row). Images for each group were taken with the objective lens set to 10× (left column), 20× (middle column), and 40× (right column). These images are representative of multiple sections from n=3 mice for PBS treated tissues and n=5 mice for EVG/NNP and EVG/BNP treated tissues.

Author Manuscript Author Manuscript Author Manuscript Author Manuscript

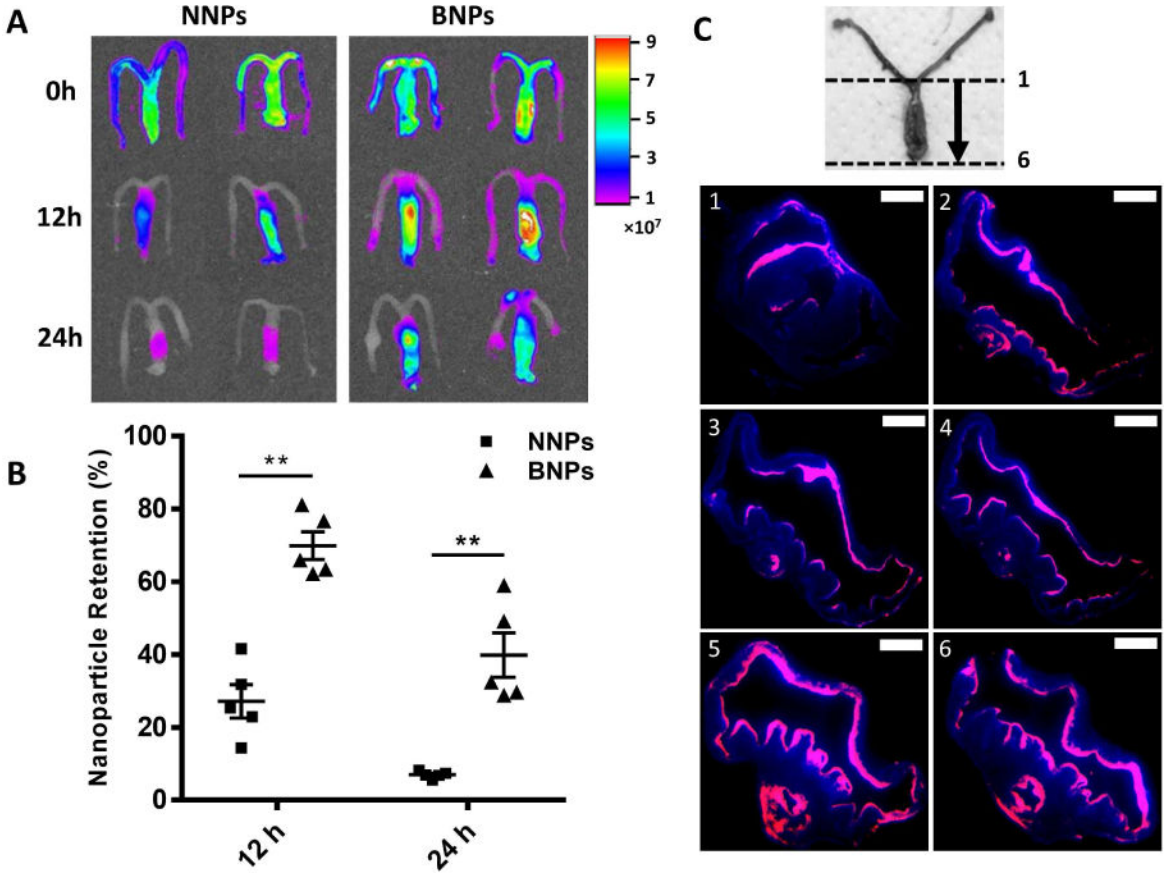


**Figure 4. Retention and distribution of nanoparticles in the reproductive tract**

A) IR imaging of harvested reproductive tissue treated with either IR-780/NNPs (left panel) or IR-780/BNPs (right panel) at 0h (top row), 12h (middle row) and 24h (bottom row). Scale bar corresponds to relative dye intensity. B) Percent retention of IR-780/NNPs and IR-780/BNPs at 12h and 24h after particle administration based on remaining fluorescence. Data is shown as mean ± SEM (n=5). Statistical significance was calculated using a Mann-Whitney U test and significance is represented on the graph as $^{**}p < 0.01$. C) Representative transverse sections of reproductive tissue 24h post treatment with DiA/BNPs. Orientation of sections is indicated in numerical order with 1 representing the most rostral and 6 representing the most caudal parts of the vaginal lumen. Pink represent fluorescent BNPs while blue represents DAPI stain. Scale bar represents 1 mm.

Author Manuscript Author Manuscript Author Manuscript Author Manuscript

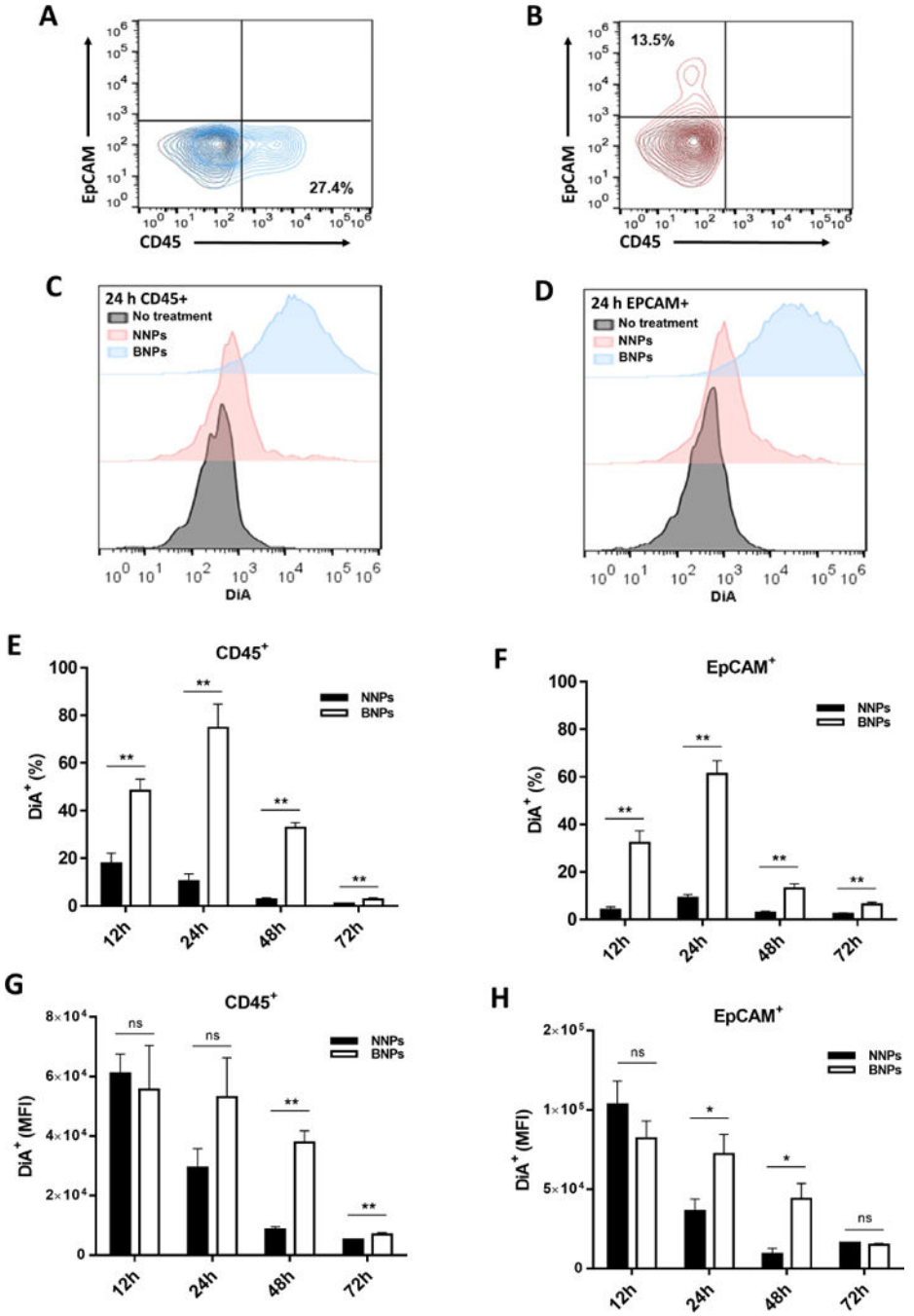


**Figure 5. Nanoparticle internalization and cell-specific association**

Gating for A) leukocytes ($CD45^+$) and B) epithelial cells ($EpCAM^+$). Black contour plots are unstained controls. Representative histogram showing DiA expression of C) $CD45^+$ and D) $EpCAM^+$ cell populations from reproductive tracts 24h post treatment with NNPs and BNPs. Positive populations from each group are in reference to untreated controls. Comparison of the percent of $DiA^+$ cells in E) $CD45^+$ and F) $EpCAM^+$ cells at 12h, 24h, 48h and 72h. MFI of G) $CD45^+$ $DiA^+$ and H) $EpCAM^+$ $DiA^+$ cell populations at 12h, 24h, 48h and 72h. Data is shown as mean ± SEM (n=5). Statistical significance was calculated

using a Mann-Whitney U test and significance is represented on the graph as ns $p > 0.05$, *$p < 0.05$, and **$p < 0.01$.

Author Manuscript Author Manuscript Author Manuscript Author Manuscript

Author Manuscript Author Manuscript Author Manuscript Author Manuscript

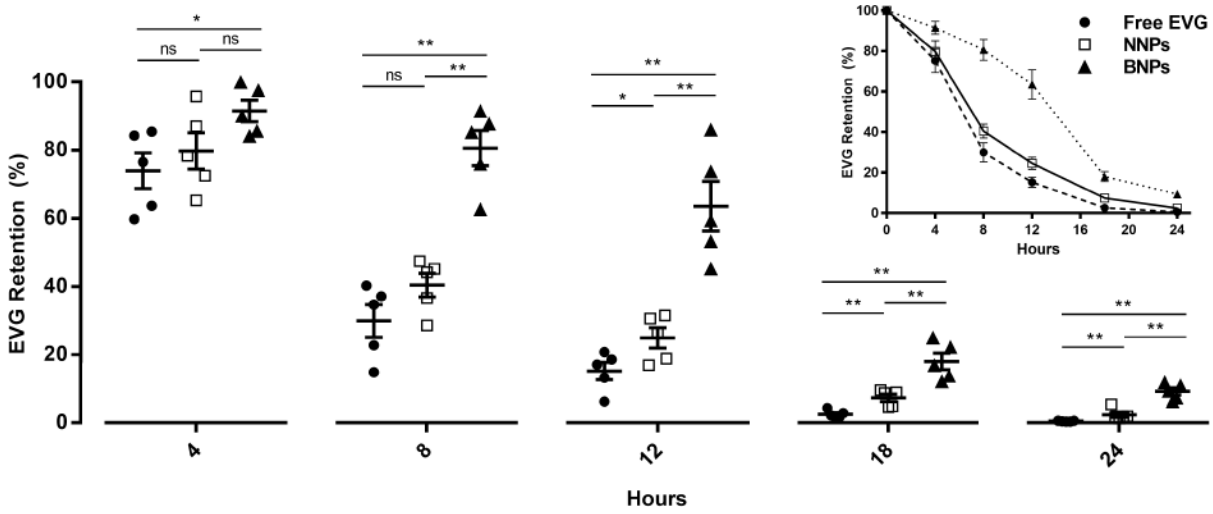


**Figure 6. EVG retention in *vivo***

Comparison of in *vivo* EVG retention percentages between free EVG, NNPs and BNPs at 4h, 8h, 12h, 18h and 24h. The insert shows the 24h EVG retention profile of free EVG, NNPs and BNPs. Data is shown as mean ± SEM (n=5). Statistical significance was calculated using a Mann-Whitney U test and significance is represented on the graph as ns $p > 0.05$, *$p < 0.05$, and **$p < 0.01$.